UDK 669.058.6: 57.012.3
Original scientific article/Izvirni znanstveni članek

ISSN 1580-2949
Mater. Tehnol.

EFFECT OF MAGNETRON SPUTTERING POWER ON THE MICROSTRUCTURE AND HYDROGEN RESISTANCE OF CrN COATINGS APPLIED WITH THE MAGNETRON SPUTTERING METHOD

VPLIV MOČI MAGNETRONSKEGA NAPRŠEVANJA NA MIKROSTRUKTURO IN ODPORNOST NA VODIK PRI KROM-NITRIDNIH PREVLEKAH

Ke Cai[1,2], Bailing Jiang[1*], Xiaolei Su[3]

[1]School of Materials Science & Engineering, Xi'an University of Technology, Shaanxi Xi'an 710048, P.R. China
[2]CNPC Tubular Goods Research Institute, Shaanxi Xi'an 710077, P.R. China
[3]School of Materials Science & Engineering, Xi'an Polytechnic University, Shaanxi Xi'an 710048, P.R. China

Prejem rokopisa – received: 2025-01-15; sprejem za objavo – accepted for publication: 2025-02-24

doi:10.17222/mit.2025.1375

CrN coatings were prepared using the magnetron sputtering method at different power levels. The prepared coatings were characterized with X-ray diffraction (XRD), and field emission scanning electron microscopy (FESEM). The electrochemical corrosion behavior and hydrogen resistance of the prepared coatings were tested using an electrochemical workstation. Results show that CrN was prepared successfully. Nanopores gradually decrease with an increase in the Cr-target power, as small hydrogen atoms pass through the gaps between the crystals and coating nanopores. When the Cr-target power was 130 W, the prepared CrN coating exhibited the densest structural features and the best hydrogen resistance.

Keywords: CrN coating, hydrogen resistance, microstructure

Avtorji so pripravili krom-nitridne (CrN) prevleke s postopkom magnetronskega naprševanja z različno močjo. Izdelane prevleke so okarakterizirali s pomočjo rentgenske difrakcijske spektroskopije (XRD) in vrstične elektronske mikroskopije na emisijo polja (FESEM). Elektrokemijsko obnašanje prevlek in odpornost na vodik so avtorji ugotavljali na elektrokemijski delovni postaji. Rezultati preiskav in analiz so pokazali, da so avtorji uspešno izdelali željene CrN prevleke. Delež in velikost nanopor v prevlekah se je postopma zmanjševal z naraščajočo močjo magnetronskega naprševanja. To je ugodno vplivalo na zmanjšanje difuzije atomov vodika skozi kristalne vrzeli in nano pore. Pri ciljani moči Cr tarče 130 W so avtorji dobili CrN prevleke z najgostejšo strukturo in najboljšo odpornost na difuzijo vodika.

Ključne besede: krom-nitridne prevleke, odpornost na vodik, mikrostruktura

1 INTRODUCTION

The presence of hydrogen in metallic materials is widely known to negatively affect the mechanical characteristics. Steel composed primarily of ferrite or martensite structures with high strength is known to have high hydrogen diffusibility and a strong tendency to suffer from hydrogen embrittlement.[1] Materials with excellent hydrogen barrier properties have become a research hotspot. The diffusion coefficient of hydrogen in ceramic materials is much lower than that in metal materials, so a layer of ceramic film can be prepared on a metal surface to suppress hydrogen diffusion.[2–4] There are currently three common types of hydrogen barrier coatings: oxide coatings (Al_2O_3, Cr_2O_3, SiO_2, ZrO_2, etc.), non-oxide coatings (TiN, SiC, AlN, CrN, etc.), and composite coatings (TiN TiC, Cr_2O_3-SiO_2, etc.). Non-oxide coatings mainly include two categories: carbides and nitrides. Among them, CrN coating is considered as one of the important materials for hydrogen barrier coatings of metal materials due to its good wear resistance, high film-substrate bonding strength, and excellent high-temperature oxidation resistance.[5,6]

Liu Liangliang et al. prepared dense CrN coatings with the magnetron sputtering deposition method to reduce the negative effect of hydrogen. The prepared CrN coatings show high compactness due to an abnormal growth of grains. Hydrogen permeation reduction of samples coated with CrN is better than that of the unprotected X70 substrate.[7] Lulu Hu et al. synthesized dense and homogeneous CrN/AlTiN nano-multilayer coatings with different period-thicknesses and studied the effect of an interface on hydrogen isotope permeation resistance. As the nano-multilayer coating contained more interfaces, it showed much higher permeation reduction factors (PRFs) than the corresponding monolayer coatings.[8] Xinyu Meng fabricated NiCr coatings with different ratios of Ni and Cr on X70 pipeline steels using mag-

*Corresponding author's e-mail:
jiangbail@vip.163.com (Bailing Jiang)

netron co-sputtering and annealing. Each coating was an adaptively grown structure with an upper Cr_2O_3 layer, outer Fe-Ni-Cr layer, and inner Fe-Ni layer formed after annealing. It showed better hydrogen permeation reduction than that of the uncoated substrate.[9] A larger Cr concentration improves the mechanical properties and corrosion resistance of NiCr coatings.

According to the above research findings, the matrix used is mainly the X70 substrate, and good hydrogen barrier performance is obtained using multi-layer CrN composite coatings. Secondly, there are few studies on the preparation of CrN hydrogen barrier coatings on X80 substrates, and the effects of preparation process parameters on their properties. A related study shows that magnetron sputtering has a significant effect on the microstructure and property of a CrN coating.[10] Therefore, in our research, CrN coatings are synthesized using magnetron sputtering at different power levels. The microstructure is characterized with XRD and SEM. Hydrogen resistance is measured using a CS2350 dual constant potential workstation and dual electrolytic cells.

2 EXPERIMENTAL PART

X80 steel was cut into pieces of (5 × 5) mm, (10 × 10) mm, (20 × 20) mm, with a diameter of 30 mm, to be used for hydrogen barrier performance testing and other microstructure testing. The substrates were polished. After polishing, all substrates were placed into a beaker containing anhydrous ethanol, and cleaned in an ultrasonic cleaning machine with a working frequency of 100 kHz and a cleaning time of 10 minutes. CrN coatings were synthesized using magnetron-sputtering equipment (MSP-300B, Beijing Chuangshiweina Technology Co., LTD., China) with power levels of (70, 90, 110 and 130) W. The flow ratio of nitrogen to argon was 4:20. The pressure in the reaction chamber was maintained at 0.3 kPa. The bias voltage value was 0 (the substrate was grounded). The deposition time was 60 min.

The phase and morphology of deposited coatings were examined using XRD (XRD-6100, SHIMADZU, Japan) and SEM (Quanta-450-FEG, FEI, American), respectively. The hydrogen diffusion coefficients of the hydrogen barrier film were measured using a CS2350 dual constant potential workstation (Wuhan Corrtest Instrument Corp., Ltd, China) and dual electrolytic cells. Each sample was used as the working electrode on both sides of the electrolytic cell, with a saturated calomel electrode as the reference electrode and a platinum electrode as the auxiliary electrode. The electrolyte for hydrogen testing was a mixed solution of 0.1 mol/L NaOH and 0.01 mol/L Na_2S, and the electrolyte for hydrogen extraction was a 0.2 mol/L NaOH solution. During testing, a constant polarization current of 10 mA was applied to the hydrogen charging side and the time was recorded. The oxidation current density was synchronously recorded on the hydrogen discharging side. Before testing, the sample was subjected to electrochemical nickel plating on the non-testing surface to prevent interference with the oxidation current measurement caused by the reactions in the stainless steel substrate during the testing process.

There are many methods for measuring the porosity of thin coatings, and calculating the porosity of thin films based on electrochemical corrosion curves is the most commonly used method.[11] This investigation used the electric method, and the calculation was as follows:

$$R(Q) = \frac{Q_{\text{Coated}}}{Q_{\text{Substrate}}} \times 100\ \% \tag{1}$$

where R (Q) is the porosity calculated with the electric quantity method, while Q_{Coated} and $Q_{\text{Substrate}}$ are the electric quantities generated by the corrosion of coated and uncoated samples in a corrosive medium within an appropriate potential range.

According to Devanathan, the time lag (t_{ag}) corresponds to the point at which $i = 0.6i\infty\text{p}$ in the hydrogen permeation current curve;[12] t_{b} is the time used for the hydrogen to pass through the sample, found by extrapolating the linear portion of the initial hydrogen permeation current transient to $i = 0$; t_{r} is the rise time constant;[6] t_{b}, t_{lag} and t_{r} were calculated according to references.[11,12] The apparent diffusion coefficient of hydrogen (D_{app}) and permeability (J) were calculated using Equations (2) and (3):[13,14]

$$D_{\text{app}} = L^2/15.3t_{\text{b}} \tag{2}$$

$$J = i\infty\text{p} \times L/F \tag{3}$$

where D_{app} (the apparent diffusion coefficient) is the hydrogen diffusion quality in 1 cm^2 per second at unit concentration gradient, J is the hydrogen permeation rate in the material, L is the thickness of the sample in cm, t_{b} is the breakthrough time (s), $i\infty\text{p}$ is the steady-state current density (μA/cm^2), and F = 96.485 C/mol (Faraday constant). According to the definitions, a longer t, smaller i, smaller D_{app} and smaller J indicate better hydrogen permeation resistance.

3 RESULTS AND DISCUSSION

Figure 1 shows XRD patterns of the prepared CrN coatings at Cr-target power levels of (70, 90, 110 and 130) W. It is evident from **Figure 1** that all diffraction peaks of the prepared samples are almost same. Diffraction peaks at 44.68° and 39.4° correspond to CrN (200) and (110). However, the (110) diffraction peaks indicate weaker intensity. In the prepared CrN coating, there are a large number of (200) oriented grains, indicating the preferential growth. When the power increases, due to the increase in the metal ion yield, the collision between N and Cr ions increases, which is more conducive to the formation of CrN, thereby promoting the crystal growth and improving the crystallinity of the thin film. Higher energy helps overcome energy barriers during crystal growth, as well as promote an ordered arrangement and

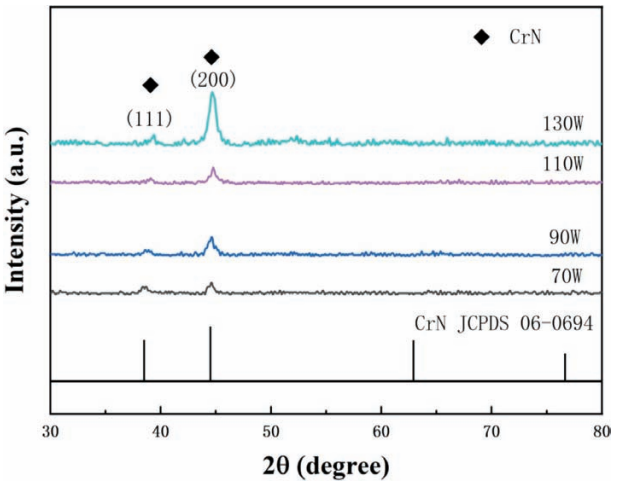

Figure 1: XRD patterns of CrN coatings prepared at different Cr-target power levels

crystal growth, thereby enhancing the intensity of diffraction peaks. In addition, moderate sputtering power also helps improve the density and grain size of the film, further enhancing the intensity of diffraction peaks. Larger grains usually lead to more pronounced diffraction effects. Therefore, as the sputtering power increases, the enhancement of diffraction peaks may indicate an improvement in the crystalline quality of the thin film.

Figure 2 shows SEM images of the prepared CrN coatings at different Cr-target power levels. As shown in this figure, a large number of particles appeared on the surfaces of CrN coatings under four different deposition conditions. When the Cr-target power is 70 W, the particles are relatively small and there are pores present. When the Cr-target power increases to 90 W, the pores gradually decrease, but the particles become larger. As the amplitude of the Cr-target power continues to increase, the number and size of large particles on the surface of the coating gradually increase. As the amplitude of the power increases, the number of large particles in the film continues to increase, but the pores gradually decrease and become denser. Increasing the sputtering power usually increases the sputtering rate of the material, resulting in more atoms or molecules desorbing from the target surface and being deposited on the substrate, thereby increasing the growth rate of the thin film. Related studies showed that when the Cr-target power is below 200 W, the crystallinity and coating integrity of the prepared CrN gradually improve with the increase in the power.[15] The thickness of CrN at a power level of 130 W is about 2.1-2.5 μm according to the cross-sec-

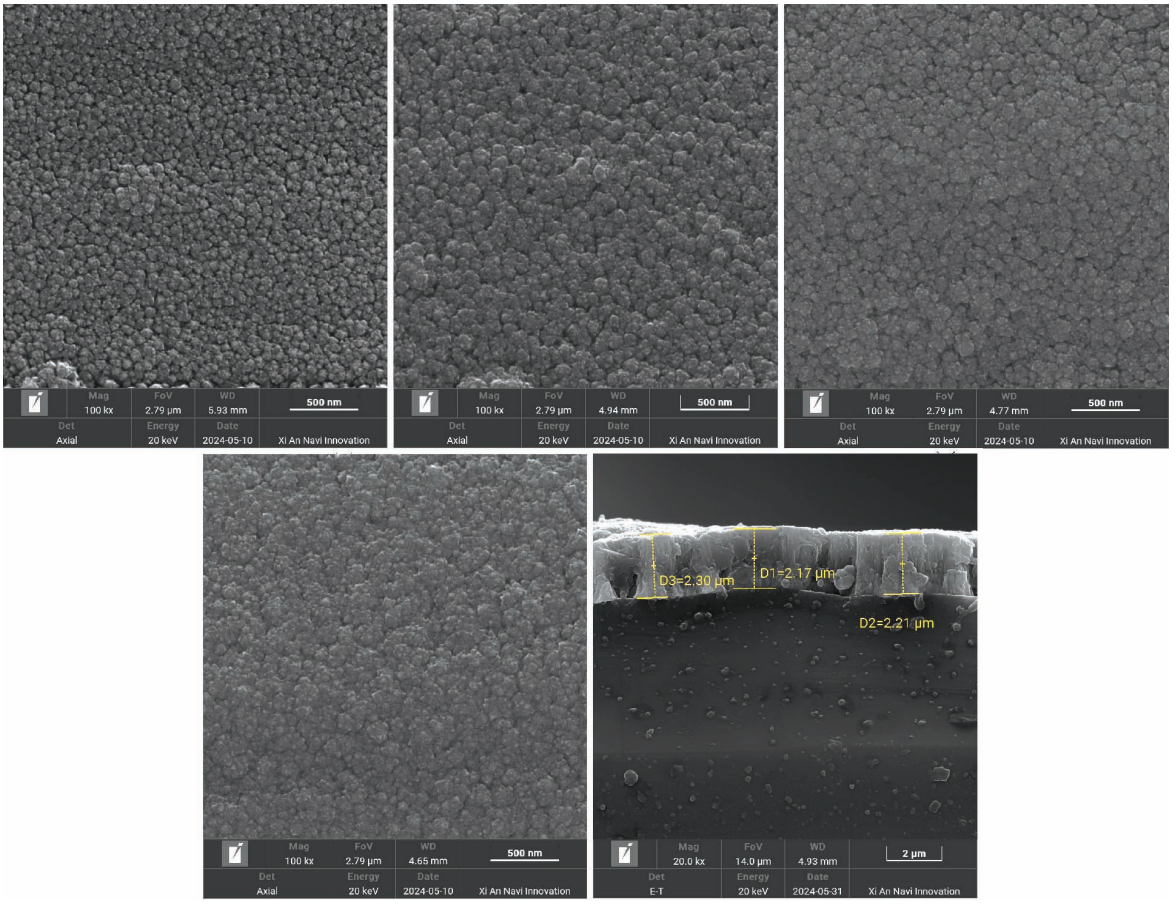

Figure 2: SEM photos and a cross-sectional image (130 W) of CrN coatings prepared at different Cr-target power levels: a) 70 W, b) 90 W, c) 110 W, d) 130 W, e) 130 W cross-sectional image

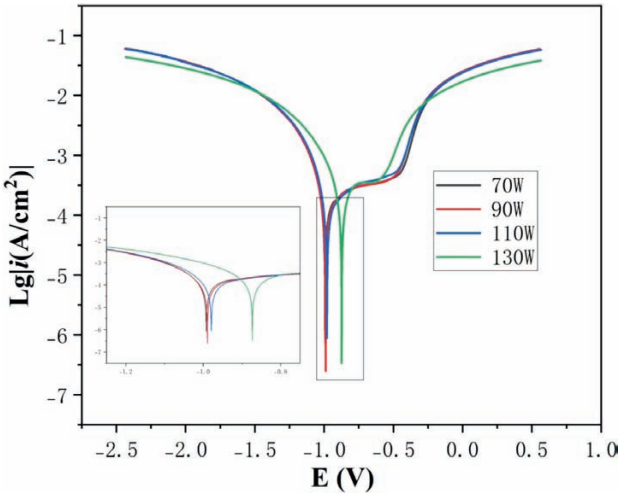

Figure 3: Dynamic polarization curves of CrN coatings prepared at different power levels

tional image. In addition, a few nanopores are observed, the reason for it being that the CrN coating was prepared using the preferential growth.

Figure 3 shows dynamic polarization curves of the CrN coatings prepared at different power levels. When the Cr-target power is low, 70 W, the corrosion potential is –0.9924V. When the Cr-target power is 90 W, the corrosion potential is –0.9891V. When the Cr-target power is 110 W, the corrosion potential is –0.9792V. When the Cr-target power increases to 130 W, its corrosion potential is –0.8732V, indicating that as the power increases, the corrosion potential gradually increases and its corrosion resistance also gradually improves. The main reason is that at low power, defects such as pores can form in the coating during the preparation process, allowing the corrosion solution to penetrate the coating. However, the coating prepared at higher power has a denser crystal structure, which greatly reduces the probability of corrosion medium penetrating the coating, thereby improving the corrosion resistance performance.[7]

Figure 4 shows porosity curves of the CrN coatings prepared at different C-target power levels. When calculating the porosity of the prepared CrN coatings, the range of natural corrosion potential selected for integration is between –1 V and –0.5 V. As –0.5 V is close to the natural corrosion potential of thin film corrosion, after the potential reaches –0.5 V, the sample begins to corrode violently. If the range taken exceeds this potential, the calculated porosity includes the porosity caused by corrosion. From **Figure 4**, it can be seen that as the Cr-target power increases, the pores in the prepared CrN coating decrease. When the Cr-target power is 130 W, the porosity of the prepared CrN coating is the lowest, about 4.35 %.

Hydrogen permeation results are displayed in **Figure 5**. The t_b indicates the time needed for hydrogen to pass through the coating substrate. The current density (i) represents the permeation rate of the hydrogen. Therefore, longer t_b and lower i indicate better hydrogen permeation resistance. **Figure 5** shows that hydrogen diffused quickly in the bare X80 substrate. Thus, the equilibrium current is high and continues to increase during the test, indicating poor hydrogen permeation resistance.

From **Figure 6**, it is clear that t_b increases with increasing power, while i decreases in the opposite direction. To quantitatively calculate D_{app} and J at 36,000s, i_t was taken as $i \propto p$. $D_{coated}/D_{substrate}$ and $J_{coated}/J_{substrate}$ increase with increasing power. This shows that hydrogen resistance increases with increasing power. When the power is 130 W, the hydrogen resistance is the best. The reason is that this high power generates a perfect coating, which is also a thicker coating. In addition, X80 steel is mainly composed of ferrite, with a small amount of pearlite and trace alloying elements. The diffusion of hydrogen atoms occurs very rapidly in ferrite, with pearlite serving as a barrier layer that can slow down the diffu-

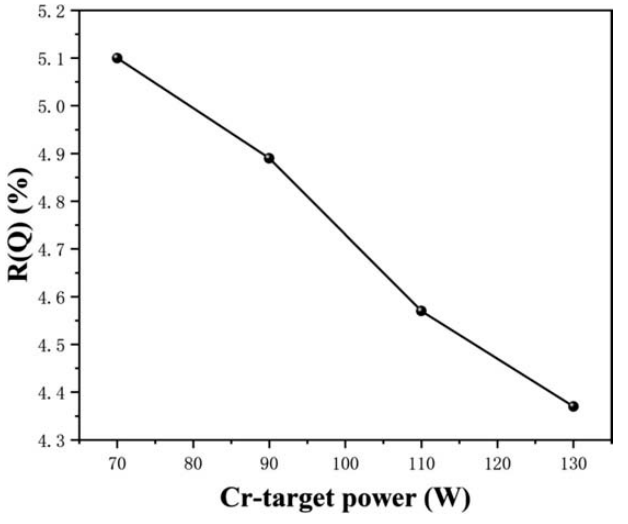

Figure 4: Porosity curves of CrN coatings prepared at different C-target power levels

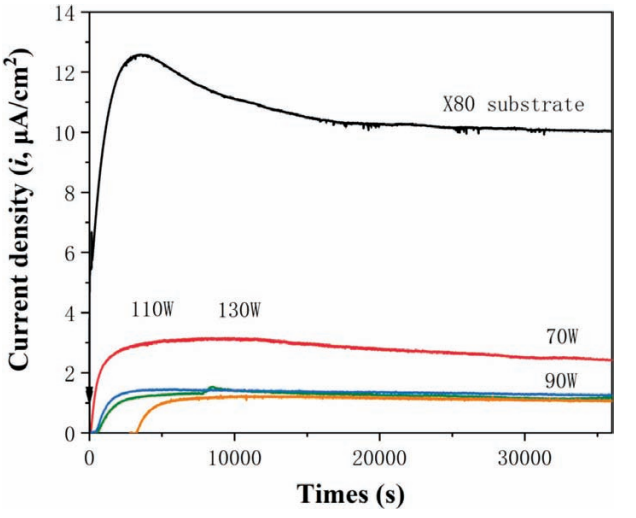

Figure 5: Electrochemical hydrogen permeation curves of CrN coatings prepared at different power levels

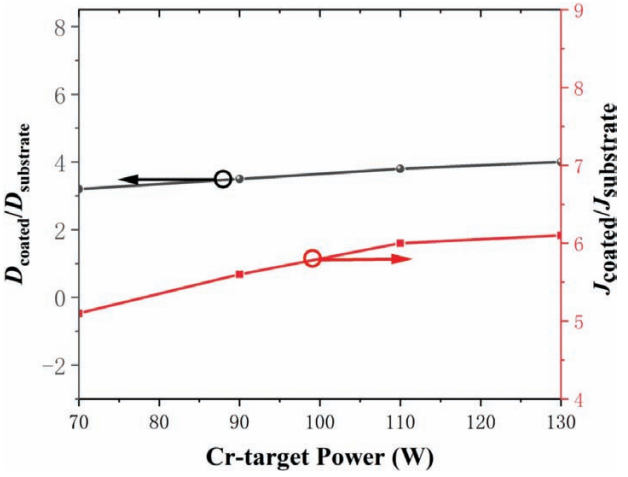

Figure 6: Improvement in D_{app} and J compared with the uncoated substrate

sion of hydrogen atoms. In CrN coatings, hydrogen diffuses in the form of hydrogen molecules through two different diffusion modes. Within the main diffusion mode, after hydrogen is adsorbed on the surface of a metal material, hydrogen molecules further decompose and enter the interior of the metal material in the atomic form for diffusion and permeation. However, after adsorption on the surface of a ceramic material, it directly dissolves into the interior of the material in the molecular form for diffusion. Due to a much larger size of hydrogen molecules compared to hydrogen atoms, the energy barrier that needs to be overcome for their migration in the same material lattice is greatly increased. Therefore, the diffusion and permeation of hydrogen inside CrN coated materials is much more difficult than in metallic materials.[16,17]

Figure 7 shows the schematic diagram of hydrogen atom permeation. A related study shows that a CrN (including (200) and (111) plane) coating is inert to hydrogen and does not adsorb hydrogen.[18] Therefore, the main infiltration method of hydrogen in CrN coatings is through defect transmission. According to the previous analysis, when the power is low, there are many nanopores in the prepared CrN coatings. These nanopores form easy paths for hydrogen to traverse to the substrate. When the power increases to 130 W, the nanopores decrase significantly and the paths for hydrogen to traverse to the substrate disappear. Nanopores decrease with increasing power, which is consistent with SEM results, while the CrN coating exhibits a dense and unique crystal structure, consistent with relevant research. The grain boundaries and atom interstice can hinder the H-atom permeation because of the larger atom size of CrN coatings. Therefore, CrN coated samples show better hydrogen permeation resistance due to the dense structure and absence of grain gaps.

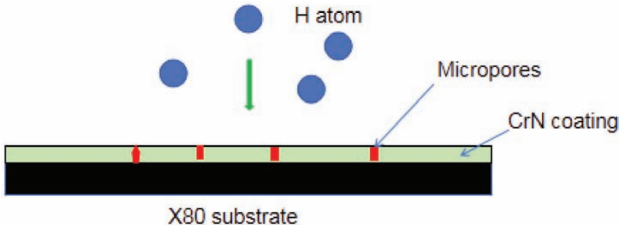

Figure 7: Schematic diagram of hydrogen atom permeation

5 CONCLUSIONS

A CrN coating was synthesized using the magnetron-sputtering method at different power levels. The prepared CrN coating exhibits preferential growth with the CrN (200) phase. As the power increases, the corrosion resistance of the CrN coating also improves due to the reduction in nanopores. The CrN (including (200) and (111) plane) coating is inert to hydrogen and does not adsorb hydrogen. Compared with the pure X80 steel substrate, the hydrogen resistance of the prepared CrN coated X80 steel is better due to a dense and unique crystal structure. The hydrogen resistance of the prepared CrN coated X80 steel increases with increasing sputtering power, due to a reduction in nanopores. When the Cr-target power is 130 W, the porosity of the prepared CrN coating is the lowest, 4.35 %, exhibiting the best hydrogen resistance.

6 REFERENCES

[1] J. A. Ronevich, B. P. Somerday, C. W. San Marchi, Effects of microstructure banding on hydrogen assisted fatigue crack growth in X65 pipeline steels, Inter. J. Fatigue, 82 (**2016**) 2, 497–504, doi:10.1016/j.ijfatigue.2015.09.004

[2] X. Xiang, X. L. Wang, G. K. Zhang, T. Tang, X. C. Lai, Preparation technique and alloying effect of aluminide coatings as tritium permeation barriers: a review, Int. J. Hydrogen Energy, 40 (**2015**), 3697–707, doi:10.1016/j.ijhydene.2015.01.052

[3] F. Franza, L. V. Boccaccini, A. Ciampichetti, M. Zucchetti, Tritium transport analysis in HCPB DEMO blanket with the FUS-TPC code, Fusion Eng. Des., 88 (**2013**), 2444–7, doi:10.1016/j.fusengdes.2013.05.045

[4] C. San Marchi, B. P. Somerday, S. L. Robinson, Permeability, solubility and diffusivity of hydrogen isotopes in stainless steels at high gas pressures, Int. J. Hydrogen Energy, 32 (**2007**), 100–16, doi:10.1016/j.ijhydene.2006.05.008

[5] L. A. Hughes, B. P. Somerday, D. K. Balch, C. San Marchi, Hydrogen compatibility of austenitic stainless steel tubing and orbital tube welds, Int. J. Hydrogen Energy, 39 (**2014**), 20585–90, doi:10.1016/j.ijhydene.2014.03.229

[6] B. P. Somerday, J. A. Campbell, K. L. Lee, J. A. Ronevich, C. San Marchi, Enhancing safety of hydrogen containment components through materials testing under in-service conditions, Int. J. Hydrogen Energy, 42 (**2017**), 7314–21, doi:10.1016/j.ijhydene.2016.04.189

[7] L. Liu, Q. Ruan, S. Xiao, X. Meng, C. Huang, Y. Wu, R. K. Y. Fu, P. K. Chu, Fabrication and hydrogen permeation resistance of dense CrN coatings, Sur. Coat. Tech., 437 (**2022**), 128326, doi:10.1016/j.surfcoat.2022.128326

[8] L. Hu, G. Wei, R. Yin, M. Hong, T. Cheng, D. Zhang, S. Zhao, B. Yang, G. Zhang, G. Cai, Y. Shi, C. Jiang, F. Ren, Significant hydrogen isotopes permeation resistance via nitride nano-multilayer coating, Int. J. Hydrogen Energy, 45 (**2020**), 19583–19589, doi:10.1016/j.ijhydene.2020.05.123

[9] X. Meng, S. Xiao, C. Wu, W. Li, S. Fan, K. Shi, P. K. Chu, Enhanced hydrogen resistance of X70 pipeline steels by adaptive growth of NiCr composite coatings with Cr/Fe_xNi_y inlaid structures, J. Alloys Comp., 997 (**2024**), 174932, doi:10.1016/j.jallcom.2024.174932

[10] V. Kouznetsov, K. Macak, J. M. Schneider, et al., A novel pulsed magnetron sputter technique utilizing very high target power densities, Surf. Coat. Tech., 122 (**1999**) 2–3, 290–293, doi:10.1016/S0257-8972(99)00292-3

[11] J. P. Celis, D. Drees, E. Maesen, J. R. Roos, Quantitative determination of through-coating porosity in thin ceramic physically vapour-deposited coatings, Thin Solid Films, 224 (**1993**) 1, 58–62, doi:10.1016/0040-6090(93)90458-2

[12] M. A. V. Devanathan, Z. Stachurski, The adsorption and diffusion of electrolytic hydrogen in palladium, Proc. R. Soc. A: Math. Phys. Eng. Sci., 27 (**1962**), 90–102, doi:10.1098/rspa.1962.0205

[13] Y. F. Cheng, Analysis of electrochemical hydrogen permeation through X-65 pipeline steel and its implications on pipeline stress corrosion cracking, Int. J. Hydrog. Energy, 32 (**2007**), 1269–1276, doi:10.1016/j.ijhydene.2006.07.018

[14] A. Turnbull, M. Maria, N. D. Thomas, The effect of H_2S concentration and pH on hydrogen permeation in AISI 410 stainless steel in 5% NaCl, Corros. Sci., 29 (**1989**), 89–104, doi:10.1016/0010-938X(89)90082-6

[15] H. J. Song, Q. Yan, The characteristics of CrN_x coatings with different interlayer, Adv. Mater. Res., 204 (**2011**), 938–941, doi:10.4028/www.scientific.net/AMR.204-210.938

[16] P. Zhou, W. Li, X. Zhu, et al., Graphene containing composite coatings as protective coatings against hydrogen embrittlement in quenching & partitioning high strength steel, J. Electrochem. Soc., 163 (**2016**), D160–D166, doi:10.1149/2.0551605jes

[17] Q. Cui, J. Wu, Effect of nanosized NbC precipitates on hydrogen diffusion in X80 pipeline steel, Mater., 10 (**2017**) 7, 721–728, doi:10.3390/ma10070721

[18] S. Fite, I. Zukerman, A. Ben Shabat, S. Barzilai, Hydrogen protection using CrN coatings: Experimental and theoretical study, Surf. Interf., 37 (**2023**), 102629, doi:10.1016/j.surfin.2023.102629